Materials Science and Engineering A 539 (2012) 107–114

Contents lists available at SciVerse ScienceDirect

Materials Science and Engineering A

journal homepage: www.elsevier.com/locate/msea

# High temperature deformation behavior of Ti–46Al–2Cr–4Nb–0.2Y alloy

Fantao Kong[a,c,*], Yuyong Chen[a], Deliang Zhang[b], Shuzhi Zhang[a]

[a] School of Materials Science and Engineering, Harbin Institute of Technology, Harbin 150001, PR China
[b] Waikato Centre for Advanced Materials, School of Engineering, The University of Waikato, Private Bag 3105, Hamilton, New Zealand
[c] State Key Laboratory of Advanced Welding Production Technology, Harbin 150001, PR China

ARTICLE INFO

*Article history:*
Received 30 March 2011
Received in revised form
30 November 2011
Accepted 17 January 2012
Available online 25 January 2012

*Keywords:*
Intermetallics
TiAl alloys
Deformation
Processing map
Forging
Microstructure

ABSTRACT

The hot deformation characteristics of cast and hot isostatically pressed Ti–46Al–2Cr–4Nb–0.2Y (at%) alloy in the temperature range of 1100–1250 °C and strain rate range of 0.01–1.0 $s^{-1}$ using hot compression tests were studied. The processing map of the alloy at true strain of 0.5 was also developed on the basis of the dynamic materials model (DMM). The experimental results show that the flow stress decreases significantly with increasing deformation temperature and decreasing strain rate. Using the kinetic rate equation the stress exponent $n$ and the apparent activation energy of deformation $Q$ were determined as 4.47 and 400.4 kJ $mol^{-1}$, respectively. The efficiency values of power dissipation of the domain at strain rate below 0.4 $s^{-1}$ show that the dynamic recrystallization occurring of $\gamma$ phase in the alloy is easier in the wide deformation temperature range (1100–1250 °C) due to low stacking fault energy. The fraction of new recrystallized grains increased with increasing the hot deformation temperature at a given strain rate. With the increasing of strain rate, the uniformity of microstructure was decreased. The domain defined by the temperature range of 1200–1230 °C and the strain rate range of 0.01–0.05 $s^{-1}$ which corresponds to a peak efficiency of about 60% is the optimal deformation condition of the alloy. Based on the optimal deformation conditions, a cylindrical sample was near isothermally forged. The microstructure and shape of pancake by forging was in good agreement with the prediction of processing map.

## 1. Introduction

$\gamma$-TiAl intermetallic based alloys are important materials for applications in making high-temperature structural components used in aerospace and automotive industries due to their high specific strength, low density, high creep resistance (in comparison with titanium alloys) and good oxidation resistance at elevated temperatures [1–4]. Among the hot forming methods of the TiAl alloys, ingot metallurgy method which is a combination of ingot casting and thermomechanical processing of the ingot is an attractive route because of the good mechanical properties, and uniform and fine microstructure of the final products. Through thermomechanical processing of TiAl alloys, different microstructures ranging from lamellar to equiaxed can be obtained [5–8]. However, TiAl alloys still generally exhibit limited hot workability at elevated temperatures that restrict them from being widely used for many desirable applications [9–11]. In this sense, establishing a processing map for a promising alloy is critically important for defining the optimum thermomechanical processing conditions within hot workability limit, and for understanding the hot deformation mechanisms and microstructure/hot deformation behavior relationships of TiAl alloys.

In recent years, processing maps have been developed based on the Dynamic Materials Model (DDM) which describes the ability of the material to dissipate power through microstructural changes during deformation processing. They have been used to evaluate the thermal deformation mechanisms of a wide range of metallic materials such as magnesium alloys, aluminum alloys, austenitic steel, Ni-based superalloys, titanium alloys as well as intermetallics [12–16]. The processing map can be obtained by combining the instability map and the power dissipation map, and used to identify the key microstructural mechanisms of hot deformation and define optimum deformation process parameters. In this study, we established the processing map for isothermal compression of a Ti–46Al–2Cr–4Nb–0.2Y (at.%) alloy with a near lamellar (NL) microstructure, and used it to determine the optimum forging condition window and achieve an indepth understanding of the deformation mechanisms and the cause for internal damage during forging. We also demonstrated the validity of the processing map by preparing a defect-free pancake of the Ti–46Al–2Cr–4Nb–0.2Y alloy by hot upset forging a canned ingot using the optimum process parameters defined by the processing map.

---

* Corresponding author at: School of Materials Science and Engineering, Harbin Institute of Technology, Harbin 150001, PR China. Tel.: +86 451 86418802; fax: +86 451 86418802.
*E-mail address:* kft@hit.edu.cn (F. Kong).

0921-5093/$ – see front matter © 2012 Elsevier B.V. All rights reserved.
doi:10.1016/j.msea.2012.01.066

## 2. Experimental procedure

A cylindrical TiAl alloy ingot (100 mm diameter × 200 mm height), with a nominal composition of Ti–46Al–2Cr–4Nb–0.2Y (in at.%), was prepared in an induction skull melting (ISM) furnace using Ti sponge (purity: 99.7 wt%), Al pieces (purity: 99.99 wt%), Cr granules (99.9 wt%) and Al–Nb and Al–Y master alloy pieces. Chemical analyses confirmed that the composition of the ingot matched the nominal composition within the experimental error. In order to eliminate the shrinkage porosity from casting, the ingot was hot isostatically pressed at 1250 °C for 4 h under a pressure of 170 MPa. The ingot was then heat treated at 950 °C for 48 h, followed by air-cooling.

Hot isothermal uniaxial compression tests were conducted using a Gleeble-1500D simulator at different temperatures with an interval of 25 °C in the range of 1100–1250 °C and with different strain rates in the range of 0.01–1.0 $s^{-1}$. The cylindrical specimens had dimensions of 8 mm in diameter and 12 mm in height, and were heated to the test temperature with a heating rate of 15 °C/s and held for 3 min at the temperature prior to the isothermal compression. All the specimens were deformed to achieve a height reduction of about 60%. To reduce die friction and ensure uniform deformation, fine graphite-base lubricant was spread onto the flat die surfaces. All the tests were performed in an argon atmosphere. In order to retain the microstructure formed in situ during deformation for subsequent microstructural characterization, the specimens were water quenched immediately after the compression tests finished. The deformed specimens were sectioned parallel to the compression axis and the surfaces of the specimens were ground and polished using the standard metallography techniques for microstructural observation.

Based the deformation behavior of the Ti–46Al–2Cr–4Nb–0.2Y alloy under different conditions, optimized deformation processing parameters were determined. A cylindrical sample (height: 100 mm; diameter: 60 mm) cut from the Ti–46Al–2Cr–4Nb–0.2Y alloy ingot was canned in a strain steel forging can. The canned ingot was near isothermally forged at 1230 °C with a height reduction of more than 75% and a strain rate range of 0.01 $s^{-1}$ to 0.1 $s^{-1}$. The forged pancake was subjected to a stress relieving treatment at 900 °C for 24 h in air. The microstructures of the compression deformed and as-forged specimens were examined using X-ray diffraction (XRD) and scanning electron microscopy (SEM).

## 3. Results and discussion

### 3.1. Microstructure and deformation behavior of the cast and hot isostatically pressed alloy

As shown in Fig. 1, the cast and hot isostatically pressed Ti–46Al–2Cr–4Nb–0.2Y alloy ingot had a near lamellar structure (NL). XRD analysis showed that the alloy was primarily composed of B2, $\alpha_2$ and $\gamma$ phases, as shown in Fig. 2. The compositions of different microstructural features revealed by the SEM examination (Fig. 1) were determined semi-quantitatively by EDX analysis, and the results are shown in Table 1. Based on the results of the EDX analysis, the phases and compositions of the microstructural features as reflected by the color contrast in the SEM backscaterred electron images were as follows: (1) the massive and strip-shaped plates of B2 phase (grey contrast in Fig. 1 as indicated by A arrows) and plates of $\gamma$ phase (dark contrast in Fig. 1 as indicated by B arrows) are distributed along the boundaries of lamellar colonies (as indicated by C arrows in Fig. 1); (2) particles of a yttrium rich phase (white particles in Fig. 1 as indicated by D arrow) were also observed at the boundaries of lamellar colonies. The average size of lamellar colonies was measured to be about 170 μm.

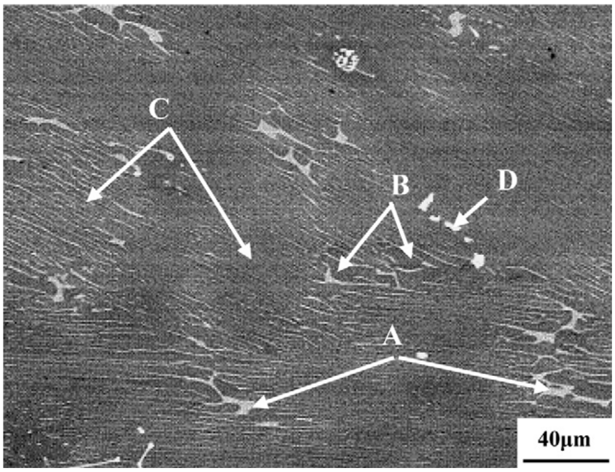

**Fig. 1.** SEM backscattered electron images showing the microstructures of the Ti–46Al–2Cr–4Nb–0.2Y alloy.

**Table 1**
The compositions of different microstructural features of Ti–46Al–2Cr–4Nb–0.2Y alloy ingot, as determined by semi-quantitative composition analysis using EDX (at.%).

| Position | Ti | Al | Cr | Nb | Y |
|---|---|---|---|---|---|
| A | 53.3 | 35.3 | 6.1 | 5.3 | 0.0 |
| B | 45.4 | 48.6 | 1.9 | 4.1 | 0.0 |
| C | 46.7 | 47.3 | 1.8 | 4.2 | 0.0 |
| D | 4.4 | 60.0 | 2.5 | 0.0 | 33.1 |

A large number of true stress-true strain curves were obtained for the Ti–46Al–2Cr–4Nb–0.2Y alloy isothermally deformed in compression with different strain rates ranging from 0.01 to 1.0 $s^{-1}$ and at different temperatures ranging from 1100 to 1250 °C. Typical stress-strain curves of the alloy deformed in $\gamma+\alpha_2$ phase field (1100 °C) and $\gamma+\alpha$ phase field (1175 °C and 1250 °C), respectively are shown in Fig. 3. The stress-strain curves showed that the flow stress was sensitively dependent on the strain rate and temperature. The flow stress increased significantly with the increase of strain rate at the same temperature, and decreased with the increase of deformation temperature at the same strain rate. All the curves exhibited initial strain hardening after yielding, and a peak flow stress at a relatively low true strain ($\leq$0.1) followed by a moderate and continuous flow softening. In addition, the stress-strain curves exhibited clear oscillation at all strain rates. The initial

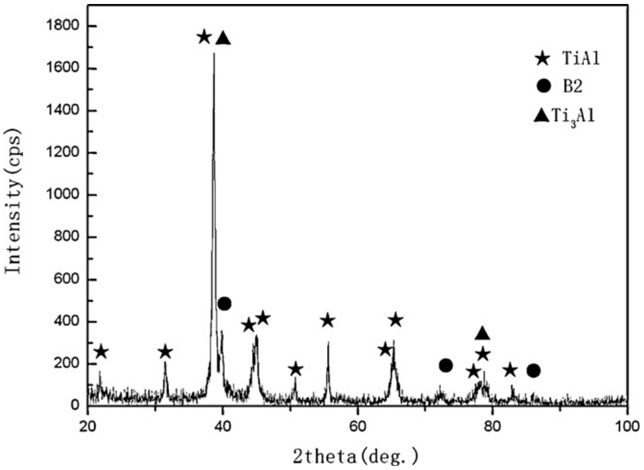

**Fig. 2.** XRD pattern of the Ti–46Al–2Cr–4Nb–0.2Y alloy.